Enhanced solar-blind responsivity of photodetectors based on cubic MgZnO films via gallium doping

Xiuhua Xie,[1,2] Zhenzhong Zhang,[1] Binghui Li,[1,*] Shuangpeng Wang,[1] Mingming Jiang,[1] Chongxin Shan,[1] Dongxu Zhao,[1] Hongyu Chen,[1,2] and Dezhen Shen[1]

[1]*State Key Laboratory of Luminescence and Applications, Changchun Institute of Optics, Fine Mechanics and Physics, Chinese Academy of Sciences, Changchun 130033, China*
[2]*University of Chinese Academy of Sciences, Beijing 100049, China*
[*]*binghuili@yeah.net*

Abstract: We report on gallium (Ga) doped cubic MgZnO films, which have been grown by metal organic chemical vapor deposition. It was demonstrated that Ga doping improves the n-type conduction of the cubic MgZnO films. A two-orders of magnitude enhancement in lateral n-type conduction have been achieved for the cubic MgZnO films. The responsivity of the cubic MgZnO-based photodetector has been also enhanced. Depletion region electric field intensity enhanced model was adopted to explain the improvement of quantum efficiency in Ga doped MgZnO-based detectors.

OCIS codes: (160.6000) Semiconductor materials; (230.0250) Optoelectronics.

References and links

1. M. Razeghi and A. Rogalski, “Semiconductor ultraviolet detectors,” J. Appl. Phys. **79**(10), 7433–7473 (1996).
2. G. Parish, S. Keller, P. Kozodoy, J. P. Ibbetson, H. Marchand, P. T. Fini, S. B. Fleischer, S. P. DenBaars, U. K. Mishra, and E. J. Tarsa, “High-performance (Al,Ga)N-based solar-blind ultraviolet p-i-n detectors on laterally epitaxially overgrown GaN,” Appl. Phys. Lett. **75**(2), 247–249 (1999).
3. E. V. Gorokhov, A. N. Magunov, V. S. Feshchenko, and A. A. Altukhov, “Solar-blind UV flame detector based on natural diamond,” Instrum. Exp. Tech. **51**(2), 280–283 (2008).
4. M. R. Luettgen, J. H. Shapiro, and D. M. Reilly, “Non-line-of-sight single-scatter propagation model,” J. Opt. Soc. Am. A **8**(12), 1964–1972 (1991).
5. Z. Xu and B. M. Sadler, “Ultraviolet communications: potential and state-of-the-art,” IEEE Commun. Mag. **46**, 6773 (2008).
6. Y. Taniyasu, M. Kasu, and T. Makimoto, “An aluminium nitride light-emitting diode with a wavelength of 210 nanometres,” Nature **441**(7091), 325–328 (2006).
7. T. Tut, M. Gokkavas, A. Inal, and E. Ozbay, “$Al_xGa_{1-x}N$-based avalanche photodiodes with high reproducible avalanche gain,” Appl. Phys. Lett. **90**(16), 163506 (2007).
8. C. J. Collins, U. Chowdhury, M. M. Wong, B. Yang, A. L. Beck, R. D. Dupuis, and J. C. Campbell, “Improved solar-blind detectivity using an $Al_xGa_{1-x}N$ heterojunction p-i-n photodiode,” Appl. Phys. Lett. **80**(20), 3754–3756 (2002).
9. G. Chen, F. Abou-Galala, Z. Y. Xu, and B. M. Sadler, “Experimental evaluation of LED-based solar blind NLOS communication links,” Opt. Express **16**(19), 15059–15068 (2008).
10. T. Li, D. J. H. Lambert, M. M. Wong, C. J. Collins, B. Yang, A. L. Beck, U. Chowdhury, R. D. Dupuis, and J. C. Campbell, “Low-noise back-illuminated $Al_xGa_{1-x}N$-Based p-i-n solar-blind ultraviolet photodetectors,” IEEE J. Quantum Electron. **37**(4), 538–545 (2001).
11. H. Srour, J. P. Salvestrini, A. Ahaitouf, S. Gautier, T. Moudakir, B. Assouar, M. Abarkan, S. Hamady, and A. Ougazzaden, “Solar blind metal-semiconductor-metal ultraviolet photodetectors using quasi-alloy of BGaN/GaN superlattices,” Appl. Phys. Lett. **99**(22), 221101 (2011).
12. Y. Koide, M. Y. Liao, and J. Alvarez, “Development of thermally stable, solar-blind deep-ultraviolet diamond photosensor,” Mater. Trans. **46**(9), 1965–1968 (2005).
13. A. Soltani, H. A. Barkad, M. Mattalah, B. Benbakhti, J. C. De Jaeger, Y. M. Chong, Y. S. Zou, W. J. Zhang, S. T. Lee, A. BenMoussa, B. Giordanengo, and J. F. Hochedez, “193 nm deep-ultraviolet solar-blind cubic boron nitride based photodetectors,” Appl. Phys. Lett. **92**(5), 053501 (2008).
14. R. Suzuki, S. Nakagomi, and Y. Kokubun, “Solar-blind photodiodes composed of a Au Schottky contact and a β-Ga_2O_3 single crystal with a high resistivity cap layer,” Appl. Phys. Lett. **98**(13), 131114 (2011).

15. K. J. Li, H. D. Liu, Q. G. Zhou, D. McIntosh, and J. C. Campbell, "SiC avalanche photodiode array with microlenses," Opt. Express **18**(11), 11713–11719 (2010).
16. P. Wang, Q. H. Zhen, Q. Tang, Y. T. Yang, L. X. Guo, K. Ding, and F. Huang, "Steady-state characteristics and transient response of MgZnO-based metal-semiconductor-metal solar-blind ultraviolet photodetector with three types of electrode structures," Opt. Express **21**(15), 18387–18397 (2013).
17. Y. Hou, Z. Mei, Z. Liu, T. Zhang, and X. Du, "$Mg_{0.55}Zn_{0.45}O$ solar-blind ultraviolet detector with high photoresponse performance and large internal gain," Appl. Phys. Lett. **98**(10), 103506 (2011).
18. S. Han, Z. Zhang, J. Zhang, L. Wang, J. Zheng, H. Zhao, Y. Zhang, M. Jiang, S. Wang, D. Zhao, C. X. Shan, B. Li, and D. Shen, "Photoconductive gain in solar-blind ultraviolet photodetector based on $Mg_{0.52}Zn_{0.48}O$ thin film," Appl. Phys. Lett. **99**(24), 242105 (2011).
19. Z. G. Ju, C. X. Shan, D. Y. Jiang, J. Y. Zhang, B. Yao, D. X. Zhao, D. Z. Shen, and X. W. Fan, "$Mg_{(x)}Zn_{(1-x)}O$-based photodetectors covering the whole solar-blind spectrum range," Appl. Phys. Lett. **93**(17), 173505 (2008).
20. S. Han, J. Zhang, Z. Zhang, Y. Zhao, L. Wang, J. Zheng, B. Yao, D. Zhao, and D. Shen, "$Mg_{0.58}Zn_{0.42}O$ Thin Films on MgO Substrates with MgO Buffer Layer," ACS Appl. Mater. Interfaces **2**(7), 1918–1921 (2010).
21. L. Wang, Z. Ju, C. Shan, J. Zheng, D. Shen, B. Yao, D. Zhao, Z. Zhang, B. Li, and J. Zhang, "MgZnO metal–semiconductor–metal structured solar-blind photodetector with fast response," Solid State Commun. **149**(45–46), 2021–2023 (2009).
22. L. K. Wang, Z. G. Ju, J. Y. Zhang, J. Zheng, D. Z. Shen, B. Yao, D. X. Zhao, Z. Z. Zhang, B. H. Li, and C. X. Shan, "Single-crystalline cubic MgZnO films and their application in deep-ultraviolet optoelectronic devices," Appl. Phys. Lett. **95**(13), 131113 (2009).
23. G. Konstantatos and E. H. Sargent, "Nanostructured materials for photon detection," Nat. Nanotechnol. **5**(6), 391–400 (2010).
24. S. Choopun, R. D. Vispute, W. Yang, R. P. Sharma, T. Venkatesan, and H. Shen, "Realization of band gap above 5.0 eV in metastable cubic-phase $Mg_xZn_{1-x}O$ alloy films," Appl. Phys. Lett. **80**(9), 1529–1531 (2002).
25. X. H. Xie, Z. Z. Zhang, B. H. Li, S. P. Wang, M. M. Jiang, C. X. Shan, D. X. Zhao, H. Y. Chen, and D. Z. Shen, "Mott-type $Mg_xZn_{1-x}O$-based visible-blind ultraviolet photodetectors with active anti-reflection layer," Appl. Phys. Lett. **102**(23), 231122 (2013).
26. L. K. Wang, Z. G. Ju, C. X. Shan, J. Zheng, B. H. Li, Z. Z. Zhang, B. Yao, D. X. Zhao, D. Z. Shen, and J. Y. Zhang, "Epitaxial growth of high quality cubic MgZnO films on MgO substrate," J. Cryst. Growth **312**(7), 875–877 (2010).
27. X. H. Xie, Z. Z. Zhang, C. X. Shan, H. Y. Chen, and D. Z. Shen, "Dual-color ultraviolet photodetector based on mixed-phase-MgZnO/i-MgO/p-Si double heterojunction," Appl. Phys. Lett. **101**(8), 081104 (2012).
28. J. Chen, W. Z. Shen, N. B. Chen, D. J. Qiu, and H. Z. Wu, "The study of composition non-uniformity in ternary MgZnO thin films," J. Phys. Condens. Matter **15**(30), L475–L482 (2003).
29. S. M. Sze, Physics of Semiconductor Devices(Wiley, 1981.)
30. T. Makino, Y. Segawa, A. Tsukazaki, A. Ohtomo, and M. Kawasaki, "Electron transport in ZnO thin films," Appl. Phys. Lett. **87**(2), 022101 (2005).
31. J. S. Liu, C. X. Shan, B. H. Li, Z. Z. Zhang, C. L. Yang, D. Z. Shen, and X. W. Fan, "High responsivity ultraviolet photodetector realized via a carrier-trapping process," Appl. Phys. Lett. **97**(25), 251102 (2010).
32. S. Han, J. Y. Zhang, Z. Z. Zhang, L. K. Wang, Y. M. Zhao, J. Zheng, J. M. Cao, B. Yao, D. X. Zhao, and D. Z. Shen, "Contact Properities of Au/$Mg_{0.27}Zn_{0.73}O$ by different annealing processes," J. Phys. Chem. C **114**(49), 21757–21761 (2010).

1. Introduction

Ultraviolet C (UVC, 100–280 nm) is a part of absent solar radiation at the Earth's surface, due to absorption in the ozonosphere [1]. The gap of solar spectrum provides a "black background" for detection of weak UVC emitting sources such as missile plume. Therefore, photodetection, with a cutoff wavelength shorter than 280 nm, has been called solar-blind photodetection [2]. Solar-blind photodetectors have found many applications including flame sensing, non-line-of-sight optical communication, missile plume sensing, UV astronomy, chemical/biological analysis, etc [3–9]. Unfortunately, the commercially available photomultiplier tubes, covering solar-blind region, have to work at high operating voltages, which limits their applications.

Currently, some wide bandgap semiconductors based detectors, focused on solar-blind sensitive, have been researched, such as $Al_xGa_{1-x}N$ [10], BGaN [11], diamond [12], cubic BN [13], monoclinic gallium oxide (β-Ga_2O_3) [14], silicon carbide [15] and $Mg_xZn_{1-x}O$ [16–18]. Among them, cubic $Mg_xZn_{1-x}O$ alloys have been receiving increasing intense attention due to its larger tunable bandgap (MgO 7.8 eV) and other unique optoelectronic natures [19–21]. Our group has obtained a responsivity of 396 mA/W under 10 V bias @ 246nm, which had been valued as one of the highest responsivity in MgZnO-based solar-blind photodetectors

[22]. On account of the consuming scattering and absorption for UVC in the ambiance, the solar-blind signal will be much weakened in a limited spread distance [4]. Accordingly, the high quantum efficiency is one of the figures of merit for solar-blind photodetectors which practice demanded [23]. However, for the cubic MgZnO based detectors, the gain mechanism is still not controllable, because of the ultra-high resistivity of the as grown films [24–26]. This is an obstacle that hampers the realization of high-performance solar-blind photodetectors. In this report, by employing Triethylgallium as the n-type dopant source, gallium (Ga) doped cubic MgZnO films have been grown by metal organic chemical vapor deposition (MOCVD). It was demonstrated through electrical, optical, and structural studies that Ga doping improves the n-type conduction of the cubic MgZnO films. An enhancement of two-orders of magnitude in lateral n-type conduction has been achieved on the cubic MgZnO films. The responsivity of the planar structure metal-semiconductor-metal (MSM) photodetector has been also enhanced. Depletion region electric field intensity (EFI) enhanced model was adopted to explain the improvement of quantum efficiency (η) in Ga doped MgZnO-based detectors.

2. Experiments and results discussion

The ~600 nm thick undoped and Ga-doped cubic MgZnO films, with the same [Mg]/[Zn] mole flow ratio, were grown on (0001) sapphire substrate by MOCVD at 450 °C, respectively. The mole flow ratio for [Ga]/([Zn] + [Mg]) was fixed in 1:500. More details about the growth conditions of cubic MgZnO can be found in our works else [25–27]. The X-ray diffraction (XRD) pattern of Fig. 1(a) reveals that the films, both undoped and Ga doped, are crystallized in cubic structure with (111) preferred orientation. There are no other significantly strong signals related to other phases, suggesting that no phase segregation or emerging of wurtzite MgZnO or Ga related spinel occurs in each MgZnO film. Both undoped and doped films have high transmission of around 80% in the visible range, and the same steep transmission edge at around 260 nm, corresponding to a bandgap of 4.77 eV, as shown in Fig. 1(b). The composition of the films is calculated to be $Mg_{0.44}Zn_{0.56}O$ from equation ($E_g = 3.02 + 4.03x$) [28].

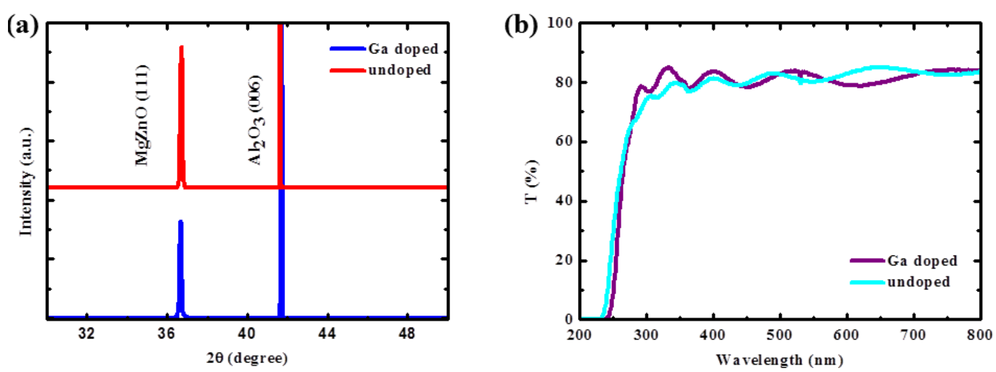

Fig. 1. (a) XRD pattern of the MgZnO films. No phase segregation is observed in both films. (b) Transmission spectrum taken from both films illustrating a bandgap of 4.77 eV, which is well within the solar-blind region.

To confirm the incorporation of Ga into cubic MgZnO films, X-ray photoelectron spectroscopy (XPS) was carried out to investigate the elemental composition of the cubic MgZnO films. For the undoped films, no XPS signals from Ga could be detected, whereas for doped films a weak peak at 20.5 eV corresponding to Ga 3d core level was observed, as can be seen in Fig. 2, in addition to the strong Mg 2p and Zn 2p signals.

As illustrated in Fig. 3(a), Au Schottky contacts, with the planar MSM structure, were fabricated on the undoped and Ga-doped cubic MgZnO films, using vacuum evaporation,

#197768 - $15.00 USD Received 17 Sep 2013; revised 2 Dec 2013; accepted 6 Dec 2013; published 2 Jan 2014

photolithography and wet etching procedure. The fingers were 500 μm long and 2 μm wide with a spacing of 5 μm. It should be noted that the Au electrodes are translucent in both the photodetectors, which will benefit to absorption of light. To explore the electrical properties, the current-voltage (I-V) curves of each photodetectors were measured in the dark. Figure 3(b) shows that the conductivity of Ga doped films is enhanced with two-orders of magnitude in lateral, which demonstrates that Ga-doping may help to make the conduction of cubic MgZnO controllable. To further contrast the optoelectronic properties of the undoped and doped samples, the photoresponse of the photodetectors was measured. As shown in Fig. 3(c), both the two photodetectors show a high sensitivity in solar-blind region. The Ga-doped sample shows an enhanced responsivity about 50 times at 265 nm under 10 V bias, compared to the undoped sample. Note that the rejection ratio of solar-blind UV to visible light, both samples, is about two orders of magnitude, demonstrating the good performance of the Ga doped cubic MgZnO. Figure 3(d) shows the responsivity as the function of bias voltage under 265 nm light illumination. In the investigated range, the Ga-doped sample always shows η is 50 times higher than the undoped sample.

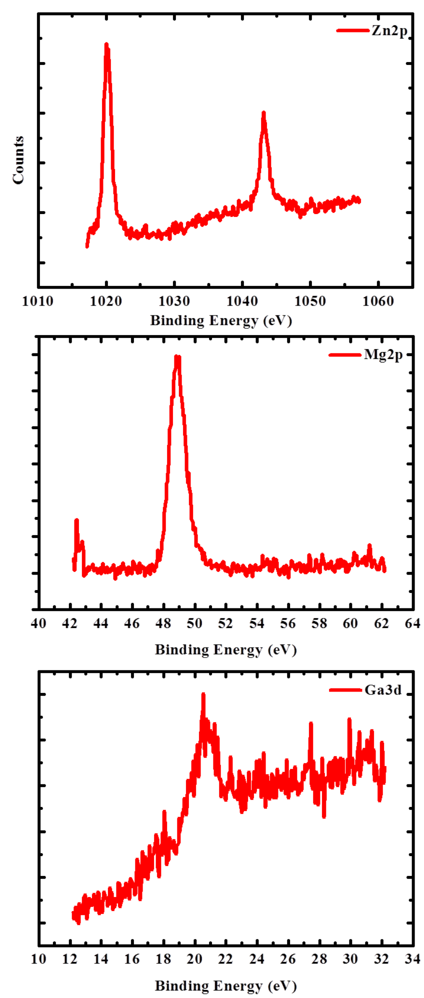

Fig. 2. XPS spectra of Ga-doped cubic MgZnO films.

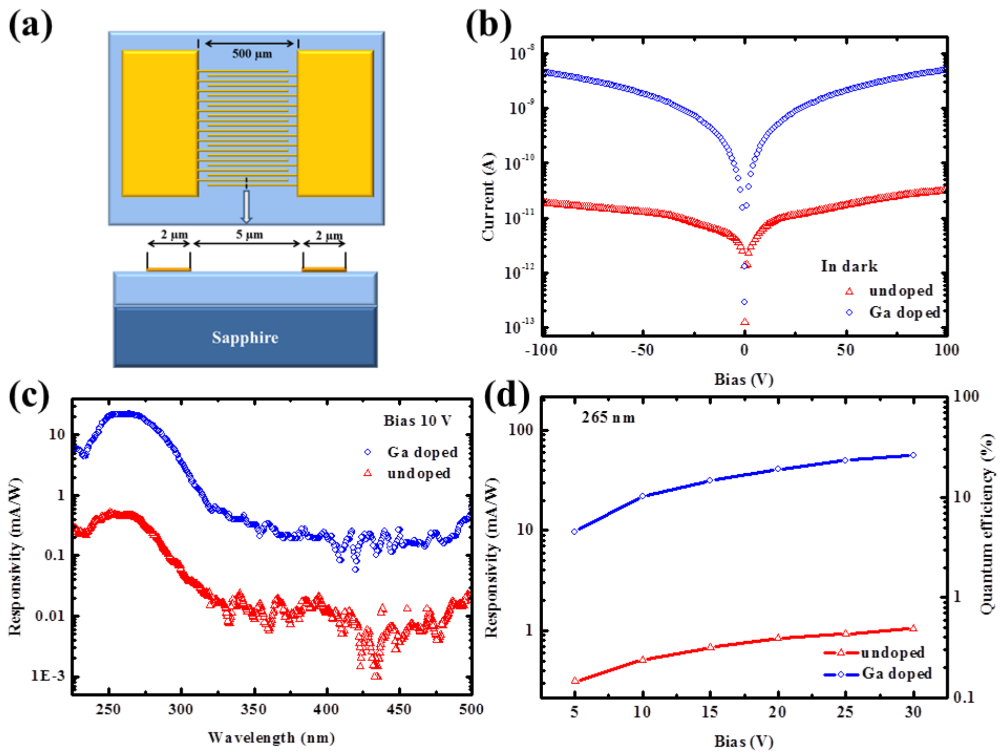

Fig. 3. (a) Schematic diagram of the MSM photodetectors. (b) I-V characteristics of the two photodetectors in dark. (c) Spectral response of the detectors at 10 V bias revealing that the devices are both blind to solar light. (d) The dependence of the maximum responsivity of the photodetectors on the external bias.

3. Theoretical modeling and simulation

The model of depletion region EFI enhanced is used to analysize the experimental results. In general, for a Schottky contact [29], if $E_{00} << k_B T$, the thermionic emission is dominated in the junction electronic transport process without tunneling, where k_B is the Boltzmann constant, T is absolute temperature, E_{00} is the characteristic energy related to the tunneling probability. E_{00} can be expressed by following formula:

$$E_{00} = (q\hbar / 2)(N / m^* \varepsilon_s)^{1/2} \tag{1}$$

where q is the elementary charge, $\hbar$ is the reduced Planck constant, N is the carrier density, m^* is the effective mass and ε_s is the relative dielectric permittivity. In this work, $m^* = 0.3m_0$ and $\varepsilon_s = 12$ for cubic MgZnO [30,31], and the carrier concentration N is about 10^{16} cm^{-3} and 10^{14} cm^{-3} for the Ga-doped and undoped films, respectively, which were estimated by the resistance of the devices. So, E_{00} is about 2.4 meV and 0.24 meV for the doped and undoped films, which are both much smaller than the thermal energy $k_B T$ at room temperature (26 meV). Therefore, the I-V curve of this Schottky contact is determined by thermionic emission model. Considering the MSM structure, consisting of two Schottky contacts connected back to back on a coplanar surface, the I-V of the detectors can be described as following:

$$\begin{gathered} I = I_s \exp(qV / nk_B T)\left[1 - \exp(-qV / k_B T)\right] \\ I_s = AA_n^* T^2 \exp(-q\phi_B / k_B T) \end{gathered} \tag{2}$$

#197768 - $15.00 USD Received 17 Sep 2013; revised 2 Dec 2013; accepted 6 Dec 2013; published 2 Jan 2014

where V is the applied bias, A is the contact area, n is the ideality factor, $q\phi_B$ is Schottky Barrier Height (SBH) and A_n* is the effective Richardson constant, which is 36 $Acm^{-2}K^{-2}$ for cubic MgZnO [32]. Then, according to the I-V curves [Fig. 3(b)], the SBH can be calculated. Here, for the doped sample, $q\phi_{B1}$ is 0.908 eV, which is almost equal to that of the undoped sample, $q\phi_{B2}$ (0.907 eV). It suggested that the built-in potential ϕ_{bi1} is equal to ϕ_{bi2}, approximately.

Meanwhile, for the Schottky contact, the depletion width (W_D) can be described as $W_D = [(2\varepsilon_s/qN_D)(\phi_{bi}\text{-}V\text{-}k_BT/q)]^{1/2}$, where N_D is the donor concentration. In this work, the N_{D1} (Ga doped sample) is larger than N_{D2} (undoped sample) by at least two-orders of magnitude, so $W_{D2}/W_{D1} \propto (N_{D1}/N_{D2})^{1/2} \geq 10$. In view of the above analysis, the Ga-doped MSM photodetector has the narrowing depletion region with the same built-in potential, which leads to a higher EFI in the effective layer. The enhanced EFI could separate the photogeneration carriers, effectively, as illustrate in Fig. 4.

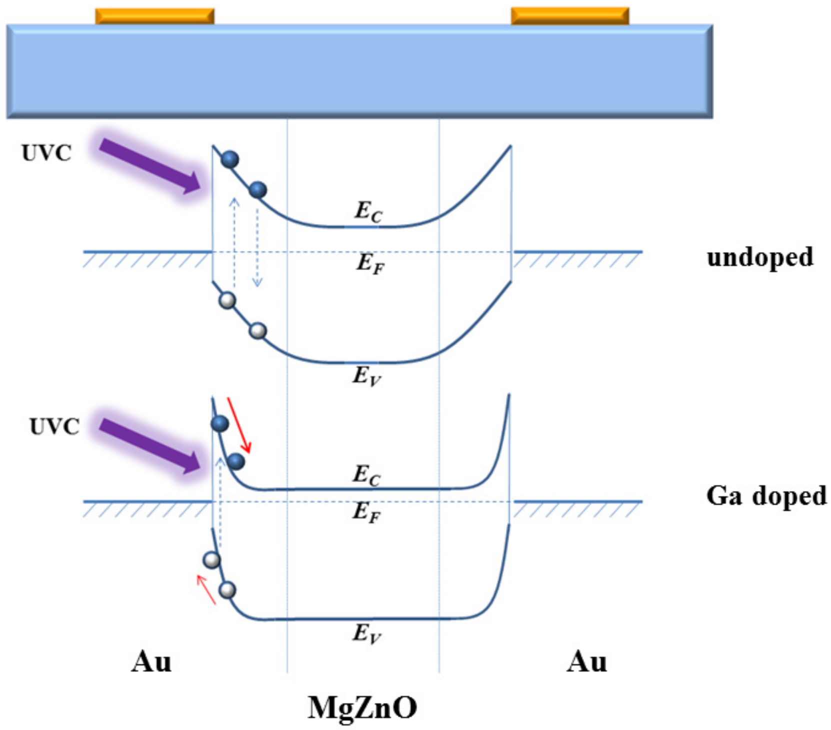

Fig. 4. Energy-band diagram of the MSM photodetectors.

To make the investigations visualized, simulations of the EFI distribution on MSM photodetectors were performed by using the COMSOL software. The proposed MSM structures and the simulation results are shown in Fig. 5. The EFI distribution, in vertical and horizontal, is shown in Figs. 5(b) and 5(c). In vertical, Ga-doped detector has a higher and abrupt EFI even reaching 600 nm. Furthermore, in horizontal, both the two detectors have the same effective EFI width. It makes sure that photogeneration carriers will be more effectively separated in the Ga-doped MSM photodetector. That is the reason why the η has been improved in the Ga doped MgZnO-based detectors.

#197768 - $15.00 USD Received 17 Sep 2013; revised 2 Dec 2013; accepted 6 Dec 2013; published 2 Jan 2014

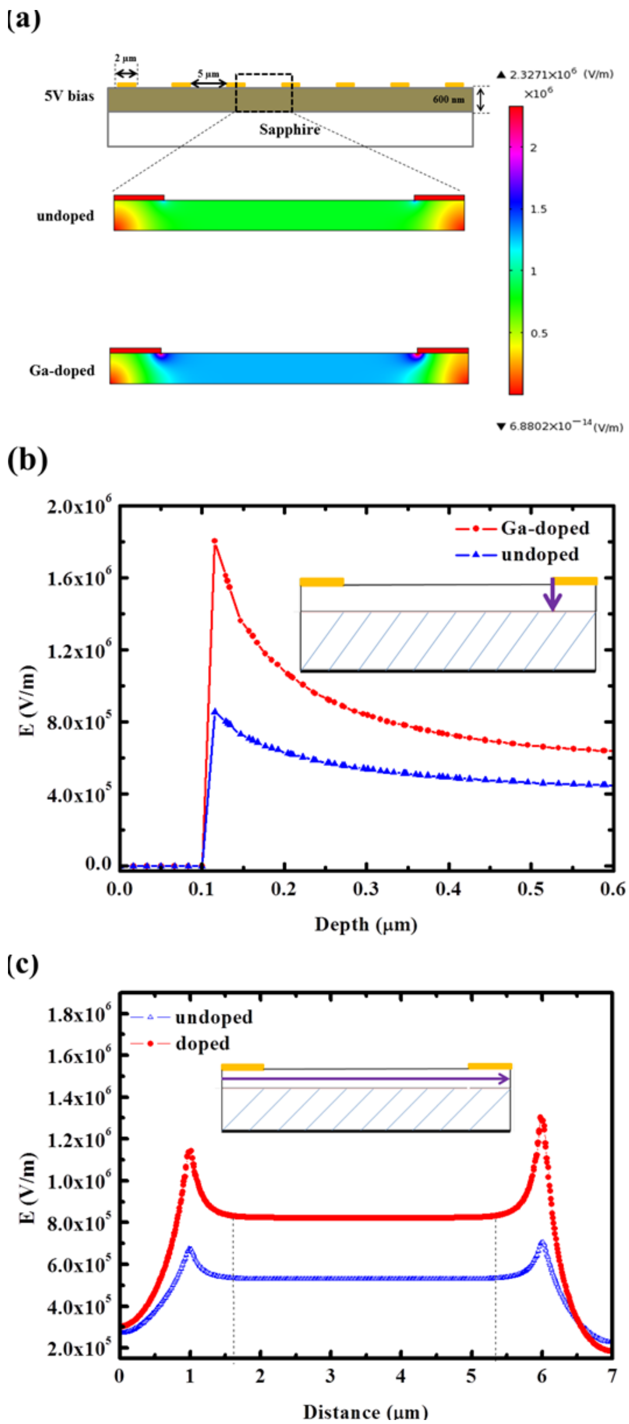

Fig. 5. Simulations of the EFI distribution on MSM photodetectors (a) whole vision, (b) in vertical, and (c) in horizontal.

4. Conclusion

In conclusion, by employing Ga-doping, the lateral conduction of cubic MgZnO films has been increased by two-orders of magnitude compared to the undoped case. The responsivity of the MSM photodetector has also been significantly improved. The EFI enhanced model was adopted to explain the improved η in the Ga-doped MgZnO-based detectors. From all the above results, it is indicated that Ga-doping (or other effective doping), which makes the electrical property of cubic MgZnO films controllable, is a valid method and prerequisite to realize the improvement of the MgZnO based photodetectors performance.

Acknowledgments

This work is supported by the National Basic Research Program of China (973 Program) under No.s 2011CB302002 and 2011CB302006, the National Natural Science Foundation of China under No.s 11134009.